Transcriptome Dynamics in Mouse Amygdala under Acute and Chronic Stress Revealed by Thio-labeled RNA Sequencing

Dan Zhao[#], Lu Zhang[#], Yang Yang[*]

School of Life Science and Technology, ShanghaiTech University, Shanghai 201210, China.

# These authors contributed equally to this work

* Correspondence: yangyang2@shanghaitech.edu.cn

Abstract

Both acute and chronic stress have significant impact on brain functions. The amygdala is essential in mediating stress responses, but how its transcriptomic dynamics change under stress remains elusive. To overcome the difficulties in detecting subtle stress-induced changes by evaluating total RNA using classic RNA sequencing, we conducted thio-labeled RNA sequencing (SLAM-seq). We injected 4-thiouridine (4sU) into mouse amygdala followed by SLAM-seq to detect nascent mRNA induced by acute and chronic restraint stress, and found that SLAM-seq could label actively transcribed genes in major neuronal and glial subtypes. We also found that acute stress induced the transcription of 6 gamma-aminobutyric acid (GABA) receptors and only 1 glutamate receptor, indicating an imminent increase of inhibitory control in the stressed amygdala. Conversely, chronic stress led to transcription of more glutamate receptors, fewer GABA receptors, and genes associated with activity-dependent myelination, suggesting a release of inhibitory control (disinhibition) and hyperactivity of the amygdala. Additionally, genes detected by SLAM-seq and RNA-seq only partially overlapped, with SLAM-seq particularly sensitive to transcriptional changes in genes with high basal transcription levels. Thus, by applying SLAM-seq *in vivo*, we obtained a rich dataset of nascently transcribed genes in the amygdala under stress, and revealed distinct transcriptional dynamics associated with acute and chronic stress.

Introduction

The impact of stress on the brain is profound and has been linked to an increased risk of mental illnesses, including depression and anxiety disorders [1, 2]. Both acute and chronic stress can induce adaptive changes in various brain regions [3-9], including the amygdala, which plays a key

role in processing physiological and behavioral responses to stress [10, 11]. In its resting state, the amygdala is tightly regulated through inhibitory mechanisms mediated by gamma-aminobutyric acid (GABA) [12]. Previous research showed that stress leads to amygdala disinhibition, resulting in its heightened activity [13, 14]. While many studies have demonstrated that stress affects amygdala function, the underlying molecular mechanisms responsible for these changes remain elusive. To understand the stress-induced effects in the amygdala at the molecular level, it is essential to study how gene expression in amygdala is influenced by acute and chronic stress.

It has long been established that neuronal activities lead to fast expression of immediate early genes, which further regulates transcription of thousands of downstream genes over an extended period [15-17]. Such activity-dependent transcription dynamics are crucial for modulating neuronal functions and long-term connectivity changes [18, 19]. Studies have shown that glial cells in the brain also exhibit significant functional changes induced by neuronal activities. For example, oligodendrocytes undergo activity-dependent myelination [20, 21]. However, the abundance of gene transcripts for maintaining cellular functions, and the complex morphology of neurons and glia, made the classic RNA sequencing (RNA-seq) method unsuitable for studying the dynamic transcriptomic changes of these cells [22].

The thio-labeled RNA sequencing (SLAM-seq) method specifically label newly transcribed mRNAs [23], and has been widely applied in cultured cells [24, 25]. Recently, SLAM-seq has also been extended to *in vivo* studies to explore genomic changes during zebrafish embryo development [26], and to identify cell type-specific transcriptome in mouse tissues in a Cre-dependent manner (SLAM-ITseq, [27]). Although SLAM-ITseq provides a solution to metabolically label RNA with 4-thiouracil (4-TU) in a specific cell type *in vivo*, this method requires usage of double-transgenic mouse lines to achieve cell type-specific expression of uracil phosphoribosyltransferase (UPRT), to transform 4-TU to 4-thiouridine (4sU) in Cre-expressing cells, limiting the applicability.

By conducting SLAM-seq with direct stereotactic injection of 4sU, we detected newly transcribed genes in the amygdala under acute and chronic stress. Bioinformatic analyses showed that the injected 4sU was integrated into the transcription of genes expressed in major brain cell types. In addition, acute stress and chronic stress induced differential transcription of GABA and glutamate

receptors, indicating diverse inhibitory control in the amygdala under acute and chronic stress. Furthermore, compared to RNA-seq, SLAM-seq is more sensitive to transcriptional changes in genes expressed in high basal levels.

Results

Adapt SLAM-seq for brain tissue analysis through stereotactic injection of 4sU

Neuronal activity is known to quickly trigger the transcription of many genes [15-17]. Seeking to detect gene transcription in response to diverse conditions of neuronal activity in different brain regions, we adapted the SLAM-seq protocol *in vivo* by injecting 4sU directly into the brain region of interest. The stereotactic injection method was used to ensure the target delivery of 4sU, a nucleotide analog that can be imported into animal cells by equilibrate nucleoside transporters [28], in selected brain regions (See Methods for details). To estimate the 4sU incorporation rate in brain cells, we first injected 4sU (100mM, dissolved in 10% DMSO, 1uL) into the mouse auditory cortex (**Fig. 1a**), and performed biotin dot blot essay with mRNAs extracted from the cortex at 2 h, 8 h, and 24 h after 4sU injection [29]. The labeling strength increased with labeling time (**Fig. 1b**), and at 24 h post injection, the labeling is highly efficient. Thus, we determined that 24 h is a sufficient duration to allow 4sU diffusion into brain cells to support SLAM-seq.

To evaluate the extent of tissue damage potentially caused by the injection of 4sU, we used TUNEL (Terminal deoxynucleotidyl transferase dUTP Nick End Labeling) staining to assess cell death in the injected brain region [30]. We injected 4sU (100mM, dissolved in 10% DMSO, 1uL) and DMSO (10%, 1uL) into the mouse auditory cortex and amygdala, and 24 h later, extracted the mouse brains for slicing and TUNEL staining (Methods). We did not see dead cells in the brain slices near the injection sites, for both 4sU and DMSO injections, suggesting that neither 4sU nor DMSO induced detectable cell death or tissue damage in the injected brain regions (**Fig. 1c, Supp. Fig. 1**).

We also assessed whether the presence of 4sU had any impact on the transcriptome by performing 150bp paired-end sequencing of total mRNA extracted from the isolated mouse auditory cortex and amygdala at 24 h after stereotactic 4sU or DMSO injections (**Supp. Fig. 2a, 2b**). By comparing the read counts for all genes [23], we did not observe any significant difference in gene expression

levels between 4sU (denoted as 4sU+) and DMSO (denoted as 4sU-) groups (**Fig.1d, Supp. Fig. 2c**). These findings support that local injection of 4sU into specific brain regions enables efficient incorporation into transcription in brain cells, without obviously affecting the gene expression.

Identify 4sU-incorporated mRNA with SLAM-seq under basal conditions

Recently, in addition to cultured cells [24, 25], SLAM-seq has also been applied *in vivo* by injecting 4sU into zebrafish embryo [26], or injecting 4-thiouracil (4-TU) intraperitoneally into transgenic mice expressing UPRT in selected cell types [27]. Given that local injection of 4sU into the mouse brain has never been reported, we needed to empirically determine whether the delivered 4sU can be incorporated into the nascently transcribed RNA molecules. We injected 4sU (100mM, 1uL, dissolved in 10% DMSO) and DMSO (10%, 1uL) into the mouse amygdala 24 h prior to tissue dissection and RNA extraction (**Fig. 2a**), to establish a baseline (BL) for nascent RNA transcription in normal behaving mice. We then subjected the aforementioned total RNA extracts to iodoacetamide (IAA) treatment (Methods, **Supp. Fig. 3a**), to covalently attach a carboxyamidomethyl group to 4sU by nucleophilic substitution [23], and then performed 150bp paired-end RNA-seq (**Supp. Fig. 3b**). During the reverse transcription step of RNA-seq library preparation, a guanine (G), instead of an adenine (A), is base paired to an alkylated 4sU, leading to the thymine (T) to cytosine (C) base conversion (T>C conversion) at the corresponding T position in mRNA [23]. To control for the background T>C conversion rate without 4sU, RNA obtained from DMSO-injected amygdala was subjected to the same procedures before RNA-seq.

We calculated the T>C conversion rates for each gene in both the 4sU-injected and DMSO-injected samples using SLAM-DUNK software [31]. At the whole transcriptome level, the average T>C conversion rate of the 4sU-injected group was significantly higher than that of DMSO-injected group (**Fig. 2b**), indicating that the injected 4sU was incorporated into transcription. We identified 414 genes with significantly higher T>C conversion rates in the 4sU group than in the DMSO group (**Fig. 2c**), which can be plausibly interpreted as genes undergoing active transcription. Note that these mice were not subjected to any behavioral or physiological perturbations, therefore, the 414 differentially 4sU-labeled genes were actively transcribed under normal baseline conditions. Indeed, these genes included sodium channels (*Scn1b*), potassium channels (*Kcnab2, Kcnc2*),

122 cation transport ATPases (*Atp1a2, Atp1b2)*, calcium channels (*Cacng7*) and Calmodulin (*Calm3*),
123 all of which are essential for maintaining basic neuronal functions [32].
124
125 **Determine the 4sU labeling efficiency in distinct cell types**
126 Identification of genes encoding neuron-specific ion channels indicated that 4sU was successfully
127 incorporated into transcription of genes in the amygdala neurons. To additionally evaluate the
128 efficiency of 4sU incorporation into the transcription of other cell types in amygdala, we cross-
129 referenced the 414 differentially 4sU-labeled genes with known marker genes of major cell types
130 as reported in single-cell RNA sequencing studies [33, 34]. We found that the 414 differentially
131 labeled genes under baseline conditions covered marker genes of excitatory (*Slc17a7, Camk2a*)
132 and inhibitory neurons (*Gad1, Gad2*), astrocytes (*Gfap, S100b*), microglia (*Fcer1g, Lyz2*) and
133 oligodendrocytes (*Mobp, Plp1*). The T>C conversion rates of these genes were significantly higher
134 in 4sU-injected than DMSO-injected amygdala (**Fig. 2d**). These results indicate that 4sU has been
135 imported into major neuronal and glial cell types of the amygdala, and could be effectively
136 incorporated into the transcription of these cells to signal nascent transcription.
137
138 **Transcriptome dynamics of the amygdala under acute stress**
139 The amygdala has been extensively implicated in stress responses [10, 11]. To identify genes that
140 were actively transcribed upon acute stress (AS), we subjected 4sU- and DMSO-injected mice to
141 1.5 h of restraint stress [35], and immediately after the stress treatment, we isolated the amygdala
142 and extracted total RNAs (Methods, **Fig. 3a**). We treated the RNA samples with IAA for SLAM-
143 seq, and identified the differentially 4sU-labeled genes using SLAM-DUNK by comparing T>C
144 conversion rates between 4sU- and DMSO-injected amygdala samples (**Supp. Fig. 4a**).
145 Meanwhile, we conducted a separate bulk RNA-seq analysis, using DESeq2 software package [36]
146 to identify differentially expressed genes (DEGs) in acute stress condition, compared to baseline.
147
148 By comparing the T>C conversion rates of genes between the 4sU and DMSO groups under AS,
149 we identified 728 differentially 4sU-labeled genes with significantly higher T>C conversion rates
150 in the 4sU group (FDR<0.05, $\log_2$FC>1, **Fig. 3b**. FDR: false discovery rate. FC: fold change). A
151 gene ontology (GO) analysis of the differentially 4sU-labeled genes in the AS samples indicated
152 enrichment for terms including "vesicle-mediated transport in synapse", "regulation of

153 neurotransmitter levels", and "synaptic vesicle cycle", all of which are closely associated with
154 synaptic vesicle functions (**Fig. 3c, Supp. Fig. 4b**). Among these are genes tightly linked to
155 synaptic vesicle release, including *Git1, Syn1, Synj1* [37-39] (**Fig. 3b**). GO analysis also revealed
156 enrichment for terms such as "regulation of synaptic plasticity" and "learning or memory", and
157 related genes included *Vgf, Prkcg, Snap25, Snap47* [40-42] (**Fig. 3b**).
158
159 A KEGG pathway analysis showed that the most significant pathways include "glutamatergic
160 synapse" and "GABAergic synapse", suggesting that AS had a strong influence on both excitatory
161 and inhibitory synaptic functions (**Fig. 3d**). Comparing genes identified under BL condition with
162 genes identified under AS, we found only one GABA receptor gene (*Gabra1*) among the
163 differentially 4sU-labeled genes under BL, in contrast to 6 GABA receptor genes under AS
164 (*Gabbr1, Gabra1, Gabra3, Gabrb2, Gabrg1, Gabrg2*), representing a higher transcription rate for
165 GABAergic receptors in the amygdala after acute stress. Conversely, only one glutamate receptor
166 gene (*Grina*) was detected under AS, and none under BL (**Fig. 3e**). Consistent with previous
167 studies linking amygdala GABAergic inhibitory control to stress response [14, 43], our results
168 suggested a strong influence on GABAergic neurons in the amygdala by acute stress, in the form
169 of quickly elevating GABA receptor expression.
170
171 **Sensitivity of SLAM-seq vs. RNA-seq**
172 Neurons require high abundance of transcripts for maintaining normal functions, while also exhibit
173 highly dynamic activity-induced transcription, making it hard to detect the subtle changes by
174 evaluating the total RNA amount using classic RNA-seq [22]. Indeed, none of the differentially
175 4sU-labeled GABA receptor and glutamate receptor genes identified by SLAM-seq were detected
176 using the differential gene expression analysis, even with a lenient standard (FDR<0.1,
177 $Log_2FC>0.1$, **Fig. 3f, Supp. Fig. 4c**). In total, 374 significantly upregulated and 279 downregulated
178 genes were identified using DESeq2 by comparing RNA read counts between AS and BL
179 conditions. 44 overlapping genes were identified by intersecting these AS-upregulated genes with
180 differentially 4sU-labeled genes under AS (**Fig. 3g**). These genes include known stress-related
181 genes such as *Cldn11, Vamp1, Glud1* and *Etnppl* [44-47]. For all of the overlapped genes, fold
182 change is bigger for SLAM-seq analysis than RNA-seq (**Fig. 3h**).
183

184 Further investigation revealed that the overlapped genes detected by SLAM-seq and RNA-seq had
185 relatively high expression levels (**Fig. 3i, Supp. Fig. 4d**). In fact, the genes with very high
186 expression levels that were marginally upregulated as determined by DESeq2 (Log_2FC <0.5) were
187 detected by SLAM-seq (red data points in **Fig. 3i**) with bigger fold changes and higher significance
188 levels (**Fig. 3h, k**). In addition, genes identified by SLAM-seq had higher expression levels than
189 genes detected by RNA-seq (**Fig. 3j**, Kolmogorov-Smirnov test, $p < 0.05$). These results suggest
190 that compared to RNA-seq, SLAM-seq is more sensitive to genes with high expression levels, and
191 is therefore useful for detecting the increased active transcription of genes that can be masked by
192 the high abundance of transcripts required for normal functioning. This is of particular importance
193 for neurons, given the high basal expression level of many genes [22].
194
195 **Transcriptome dynamics of amygdala under chronic stress**
196 Chronic stress (CS) poses prolonged impact in the brain [48]. For chronic stress experiments, we
197 subjected mice to 7 days of restraint stress, 2 h each day [49, 50] (Methods, **Fig. 4a**). To examine
198 the long-lasting transcriptomic changes under CS, we extracted the amygdala at 10 h after the final
199 restraint stress session on day 7. We reasoned that by shifting 10 h, we reduced the possibility of
200 detecting acute changes induced by the last session of restraint stress. 4sU was injected into the
201 amygdala 24 h before brain extraction, same as BL and AS experiments. By comparing T>C
202 conversion rates between 4sU and DMSO injected groups, we identified 815 differentially 4sU-
203 labeled genes under CS (**Fig. 4b, Supp. Fig. 5a**). We performed a GO analysis for these genes,
204 and found that in addition to terms associated with neuronal functions such as "synaptic vesicle
205 cycle" and "neurotransmitter secretion", there is also enrichment for terms closely linked to glial
206 cells, especially oligodendrocytes and microglia (**Fig. 4c**). These terms include "myelination",
207 "ensheathment of neurons" and "axon ensheathment", which are tightly linked to the function of
208 oligodendrocytes, as well as "autophagy" and "autophagosome", which are associated with
209 microglia (**Supp. Fig. 5b**). Among these genes, *Mag* and *Dag1* are associated with myelination,
210 and *Rragb* and *Usp36* are associated with autophagy [51].
211
212 Regarding sensitivity for SLAM-seq vs. RNA-seq, we noted a similar trend for CS data to AS.
213 DESeq2 analysis detected 53 significantly up-regulated and 11 down-regulated genes for CS
214 (FDR<0.1, Log_2FC>0.1, **Fig. 4d**). Intersection of the differentially 4sU-labeled genes identified

215 by SLAM-seq and upregulated genes identified by RNA-seq revealed 11 overlapping genes (**Fig.**
216 **4e**), all with high expression levels (**Fig. 4f, Supp. Fig. 5c**). Expression of six out of the 11
217 overlapped genes is affected by chronic stress (*Esrrg, Gabarapl2, Cct8, Vamp1, Nrsn1, Cplx1*) [47,
218 52-54]. These genes all show bigger fold changes and 9 out of 11 genes also show higher
219 significance levels for SLAM-seq than for RNA-seq (**Fig. 4h, 4i**). Similar to AS, genes identified
220 by SLAM-seq in CS also had higher expression levels (**Fig. 4g**, Kolmogorov-Smirnov test, $p <$
221 0.05), again demonstrating the sensitivity of SLAM-seq for detecting actively transcribed genes
222 with high abundance. The GO analysis of the genes identified by SLAM-seq indicated enrichment
223 for terms closely linked to glial functions, but these terms did not show in GO analysis of genes
224 identified by RNA-seq (**Supp. Fig. 6**). Thus, the low-magnitude yet persistent transcriptome
225 changes associated with CS are more likely to be captured by SLAM-seq.
226
227 **Comparison of differentially 4sU-labeled genes among BL, AS and CS conditions**
228 By comparing the differentially 4sU-labeled genes under BL, AS and CS conditions, we found that
229 a majority of genes (363 out of 413) labeled under BL were also identified in either AS or CS
230 conditions, including known housekeeping genes such as *Sdha, Ywhaz*, *Gfap* [55] (**Fig. 5a**). These
231 genes were actively transcribed regardless of stress conditions, indicating their important roles in
232 maintaining normal cellular functions. In contrast to BL, we identified many more condition-
233 specific genes after stress treatments, namely, 224 AS-specific genes and 333 CS-specific genes
234 (**Fig. 5a**). Among the 172 AS-CS overlapped genes, 29 were associated with synaptic transmission,
235 synaptic vesicle cycle and synaptic regulations (**Fig. 5a**). Thus, both acute and chronic stress
236 strongly affected synaptic functions in amygdala neurons. Notably, compared to CS, AS triggered
237 active transcription of a higher proportion of synapse-related genes, among which were genes
238 associated with protein localization to postsynaptic membrane (*Git1, Mapk10, Stx1b, Kif1a*) [39,
239 56, 57], highlighting immediate postsynaptic plasticity caused by acute stress (**Fig. 5b**).
240
241 As described in an earlier section, we detected 6 GABA receptor genes (*Gabbr1, Gabra1, Gabra3,*
242 *Gabrb2, Gabrg1, Gabrg2*) and 1 glutamate receptor gene (*Grina*) under AS, representing an
243 imminent effect of AS on GABAergic inhibitory control of the amygdala. In comparison, we found
244 4 GABA receptor genes (*Gabbr1, Gabra1, Gabra3, Gabrg2*) and 3 glutamate receptor genes
245 (*Gria3, Gria4, Grina*) among the differentially 4sU-labeled genes under CS (**Fig. 5c**). The increase

246 in excitatory receptor transcription and relatively lower transcription of GABAergic receptors
247 might underlie hyperactivity of the amygdala, caused by stress-induced removal of GABAergic
248 inhibitory control [13, 14]. In line with these findings, CS-specific genes included a larger
249 proportion of genes related to myelination, such as *Fyn, Dag1, Mag, Epb41l3,* and *Ndrg1,* and the
250 enriched GO terms included "myelination", "positive regulation of myelination", and "myelin
251 sheath" (**Fig. 5d**). Recent studies suggested that neuronal and axonal activity could trigger
252 myelination [20, 21], a phenomenon known as "activity-dependent myelination". Therefore, these
253 results suggested that chronic stress could lead to hyperactivity of amygdala neurons, as shown by
254 decreased transcription in GABAergic receptors, increased transcription in glutamatergic receptors,
255 and increased transcription in genes composing the myelin sheath.
256
257 **Discussion**
258 By directly injecting 4-sulfuridine (4sU) into the amygdala followed by SLAM-seq, we were able
259 to identify newly transcribed genes under acute and chronic stress. By cross-referencing these
260 genes with known cell type-specific marker genes, we found that the injected 4sU was integrated
261 into the transcription of major subtypes of neurons and glia cells in the amygdala. Analyses
262 revealed that acute stress resulted in increased transcription of GABA receptors in neurons, while
263 chronic stress had a stronger impact on transcription of glutamate receptors and genes associated
264 with myelination, both in line with heightened activity of the amygdala [14]. Furthermore, we
265 observed that SLAM-seq exhibited greater sensitivity to transcriptional changes in genes with high
266 expression levels compared to RNA-seq. Thus, by applying SLAM-seq to the amygdala, we
267 generated a rich dataset which can be used in future studies to dissect the functions of genes related
268 to stress responses.
269
270 Neurons have highly specialized morphology, including axons and dendrites that can span long
271 distances, with functional subcellular compartments such as dendritic spines and axonal boutons
272 [58]. The transcriptional networks in neurons are dynamically modulated by synaptic activities,
273 through coupling of a small subset of active synapses to the nucleus [59, 60]. Given the abundance
274 of gene transcripts for maintaining fundamental neuronal functions such as action potential firing
275 [19], the transcriptional modulation that lead to activation of relevant gene expression may not
276 alter the total mRNA of these genes [22]. Therefore, the most common method for gene expression

277 profiling, RNA-seq, may not be suited for accessing the highly dynamic transcriptional changes
278 under fast-varying physiological, behavioral or pathological conditions.
279
280 SLAM-seq, a metabolic RNA labeling method for identifying newly synthesized RNA molecules,
281 is an alternative approach to gain insights into the transcriptional regulation regardless of the
282 steady-state abundance of genes [24-26]. A previously published method, SLAM-ITseq, extended
283 SLAM-seq to mouse tissues by crossing Cre-dependent UPRT mice with Cre lines [27]. This
284 method requires usage of transgenic animals, and the cell types that can be investigated are
285 restricted by available Cre lines. Instead of intravenously injecting 4-thiouracil and relying on Cre-
286 dependent UPRT expression for cell-specific labeling, we used stereotactic 4sU injection to target
287 all cell types in selected brain regions. Our data showed that 4sU can be effectively imported into
288 major cell types [28], and incorporated into the transcription, without causing detectable tissue
289 damage or cell death. This is a simplified method that can be applied to any brain region in mice
290 and possibly other species using stereotaxic injection, without the need for transgenic animals.
291
292 We used this method to investigate the RNA dynamics of a key brain region involved in stress
293 conditions, the amygdala, under acute and chronic restraint stress. We found partial overlap in
294 genes detected by SLAM-seq and RNA-seq, and over half of the overlapped up-regulated genes
295 under CS condition had been implicated in chronic stress by previous studies [52-54, 61-64].
296 Notably, for all these genes, SLAM-seq showed higher sensitivity than RNA-seq, shown by higher
297 fold changes and significance levels. The upregulated genes with high abundance were detected
298 by SLAM-seq with high significance level, while barely meets the lenient criteria in RNA-seq. It
299 supports the notion that for genes with high expression rate, under physiological condition
300 (restraint stress) may not cause a noticeable change in the total amount of mRNA for relevant
301 genes. And in these situations, SLAM-seq serves as a better method for screening the highly
302 expressed genes.
303
304 Using SLAM-seq, we identified 6 GABA receptors under AS, compared to 1 under BL and 4 under
305 CS, suggesting an imminent inhibition drive induced by AS. Conversely, 3 glutamate receptors
306 were identified under CS, while only 1 under AS and 0 under BL, suggesting an increase in
307 elevated activity of the amygdala. Furthermore, CS also induced transcription of many genes

associated with myelination. Myelination has been shown to be initiated by neuronal activities [20, 21], and can in turn facilitate signal transduction in neurons [51, 65]. These results are consistent with previous findings that stress could cause hyperactivity of the amygdala [14, 66, 67]. Therefore, our findings indicated that acute and chronic stress could differentially modulate the transcription level of GABA and glutamate receptors as well as proteins constituting the myelin sheath, and in turn influence the excitation-inhibition balance of the amygdala neurons.

We provided a rich dataset of molecular responses of amygdala to acute and chronic stress, and future studies are needed to further investigate the functions of these genes.

Acknowledgements

We thank Drs. Margaret Ho and Dan-Qian Liu for comments on the manuscript. We thank Dr. Hao Wu and Ms. Liang He for assistance in data analysis and experiments. We thank the animal facility of ShanghaiTech for their excellent care of mice. This work was supported by grants from the Ministry of Science and Technology of China (2022ZD0204900), Central Guidance on Local Science and Technology Development Fund (YDZX20233100001002), and ShanghaiTech University Startup Fund to Y.Y.

References

1. Caspi, A., et al., *Influence of life stress on depression: moderation by a polymorphism in the 5-HTT gene.* Science, 2003. **301**(5631): p. 386-9.
2. Weger, M. and C. Sandi, *High anxiety trait: A vulnerable phenotype for stress-induced depression.* Neurosci Biobehav Rev, 2018. **87**: p. 27-37.
3. de Kloet, E.R., M. Joëls, and F. Holsboer, *Stress and the brain: from adaptation to disease.* Nat Rev Neurosci, 2005. **6**(6): p. 463-75.
4. McEwen, B.S., *Physiology and neurobiology of stress and adaptation: central role of the brain.* Physiol Rev, 2007. **87**(3): p. 873-904.
5. Xiao, Q., et al., *A new GABAergic somatostatin projection from the BNST onto accumbal parvalbumin neurons controls anxiety.* Mol Psychiatry, 2021. **26**(9): p. 4719-4741.
6. Davis, M., et al., *Phasic vs sustained fear in rats and humans: role of the extended amygdala in fear vs anxiety.* Neuropsychopharmacology, 2010. **35**(1): p. 105-35.
7. Mah, L., C. Szabuniewicz, and A.J. Fiocco, *Can anxiety damage the brain?* Curr Opin Psychiatry, 2016. **29**(1): p. 56-63.
8. Liu, W.Z., et al., *Identification of a prefrontal cortex-to-amygdala pathway for chronic stress-induced anxiety.* Nat Commun, 2020. **11**(1): p. 2221.
9. Liu, T., et al., *Stress induces microglia-associated synaptic circuit alterations in the dorsomedial prefrontal cortex.* Neurobiol Stress, 2021. **15**: p. 100342.
10. Roozendaal, B., B.S. McEwen, and S. Chattarji, *Stress, memory and the amygdala.* Nat Rev Neurosci, 2009. **10**(6): p. 423-33.
11. Zhang, J.Y., et al., *Chronic Stress Remodels Synapses in an Amygdala Circuit-Specific Manner.* Biol Psychiatry, 2019. **85**(3): p. 189-201.
12. Quirk, G.J. and D.R. Gehlert, *Inhibition of the amygdala: key to pathological states?* Ann N Y Acad Sci, 2003. **985**: p. 263-72.
13. Liu, Z.P., et al., *Chronic stress impairs GABAergic control of amygdala through suppressing the tonic GABAA receptor currents.* Mol Brain, 2014. **7**: p. 32.
14. Zhang, X., et al., *Stress-Induced Functional Alterations in Amygdala: Implications for Neuropsychiatric Diseases.* Front Neurosci, 2018. **12**: p. 367.

354 15. Herdegen, T. and J.D. Leah, *Inducible and constitutive transcription factors in the*
355 *mammalian nervous system: control of gene expression by Jun, Fos and Krox, and*
356 *CREB/ATF proteins.* Brain Res Brain Res Rev, 1998. **28**(3): p. 370-490.
357 16. O'Donovan, K.J., et al., *The EGR family of transcription-regulatory factors: progress at*
358 *the interface of molecular and systems neuroscience.* Trends Neurosci, 1999. **22**(4): p. 167-
359 73.
360 17. West, A.E. and M.E. Greenberg, *Neuronal activity-regulated gene transcription in synapse*
361 *development and cognitive function.* Cold Spring Harb Perspect Biol, 2011. **3**(6).
362 18. Gallo, F.T., et al., *Immediate Early Genes, Memory and Psychiatric Disorders: Focus on*
363 *c-Fos, Egr1 and Arc.* Front Behav Neurosci, 2018. **12**: p. 79.
364 19. Yap, E.L. and M.E. Greenberg, *Activity-Regulated Transcription: Bridging the Gap*
365 *between Neural Activity and Behavior.* Neuron, 2018. **100**(2): p. 330-348.
366 20. Mount, C.W. and M. Monje, *Wrapped to Adapt: Experience-Dependent Myelination.*
367 Neuron, 2017. **95**(4): p. 743-756.
368 21. Fields, R.D., *A new mechanism of nervous system plasticity: activity-dependent*
369 *myelination.* Nat Rev Neurosci, 2015. **16**(12): p. 756-67.
370 22. Lee, P.R. and R.D. Fields, *Activity-Dependent Gene Expression in Neurons.* Neuroscientist,
371 2021. **27**(4): p. 355-366.
372 23. Herzog, V.A., et al., *Thiol-linked alkylation of RNA to assess expression dynamics.* Nat
373 Methods, 2017. **14**(12): p. 1198-1204.
374 24. Alalam, H., J.A. Zepeda-Martinez, and P. Sunnerhagen, *Global SLAM-seq for accurate*
375 *mRNA decay determination and identification of NMD targets.* RNA, 2022. **28**(6): p. 905-
376 915.
377 25. Muhar, M., et al., *SLAM-seq defines direct gene-regulatory functions of the BRD4-MYC*
378 *axis.* Science, 2018. **360**(6390): p. 800-805.
379 26. Bhat, P., et al., *SLAMseq resolves the kinetics of maternal and zygotic gene expression*
380 *during early zebrafish embryogenesis.* Cell Rep, 2023. **42**(2): p. 112070.
381 27. Matsushima, W., et al., *SLAM-ITseq: sequencing cell type-specific transcriptomes without*
382 *cell sorting.* Development, 2018. **145**(13).
383 28. Yao, S.Y., et al., *Nucleobase transport by human equilibrative nucleoside transporter 1*
384 *(hENT1).* J Biol Chem, 2011. **286**(37): p. 32552-62.

385 29. Radle, B., et al., *Metabolic labeling of newly transcribed RNA for high resolution gene*
386 *expression profiling of RNA synthesis, processing and decay in cell culture.* J Vis Exp,
387 2013(78).
388 30. Gorczyca, W., et al., *Presence of DNA strand breaks and increased sensitivity of DNA in*
389 *situ to denaturation in abnormal human sperm cells: analogy to apoptosis of somatic cells.*
390 Exp Cell Res, 1993. **207**(1): p. 202-5.
391 31. Neumann, T., et al., *Quantification of experimentally induced nucleotide conversions in*
392 *high-throughput sequencing datasets.* BMC Bioinformatics, 2019. **20**(1): p. 258.
393 32. Goaillard, J.M. and E. Marder, *Ion Channel Degeneracy, Variability, and Covariation in*
394 *Neuron and Circuit Resilience.* Annu Rev Neurosci, 2021. **44**: p. 335-357.
395 33. Hochgerner, H., et al., *Neuronal types in the mouse amygdala and their transcriptional*
396 *response to fear conditioning.* Nat Neurosci, 2023. **26**(12): p. 2237-2249.
397 34. Yao, Z., et al., *A high-resolution transcriptomic and spatial atlas of cell types in the whole*
398 *mouse brain.* Nature, 2023. **624**(7991): p. 317-332.
399 35. Li, S., et al., *Effects of acute restraint stress on different components of memory as assessed*
400 *by object-recognition and object-location tasks in mice.* Behav Brain Res, 2012. **227**(1): p.
401 199-207.
402 36. Love, M.I., W. Huber, and S. Anders, *Moderated estimation of fold change and dispersion*
403 *for RNA-seq data with DESeq2.* Genome Biol, 2014. **15**(12): p. 550.
404 37. Baldelli, P., et al., *Lack of synapsin I reduces the readily releasable pool of synaptic vesicles*
405 *at central inhibitory synapses.* J Neurosci, 2007. **27**(49): p. 13520-31.
406 38. Trapani, J.G., et al., *Synaptojanin1 is required for temporal fidelity of synaptic transmission*
407 *in hair cells.* PLoS Genet, 2009. **5**(5): p. e1000480.
408 39. Montesinos, M.S., et al., *Presynaptic Deletion of GIT Proteins Results in Increased*
409 *Synaptic Strength at a Mammalian Central Synapse.* Neuron, 2015. **88**(5): p. 918-925.
410 40. Jurado, S., et al., *LTP requires a unique postsynaptic SNARE fusion machinery.* Neuron,
411 2013. **77**(3): p. 542-58.
412 41. Irfan, M., et al., *SNAP-25 isoforms differentially regulate synaptic transmission and long-*
413 *term synaptic plasticity at central synapses.* Sci Rep, 2019. **9**(1): p. 6403.

414 42. Bozdagi, O., et al., *The neurotrophin-inducible gene Vgf regulates hippocampal function*
415 *and behavior through a brain-derived neurotrophic factor-dependent mechanism.* J
416 Neurosci, 2008. **28**(39): p. 9857-69.
417 43. Andolina, D., et al., *Prefrontal/amygdalar system determines stress coping behavior*
418 *through 5-HT/GABA connection.* Neuropsychopharmacology, 2013. **38**(10): p. 2057-67.
419 44. Flati, T., et al., *A gene expression atlas for different kinds of stress in the mouse brain.* Sci
420 Data, 2020. **7**(1): p. 437.
421 45. Kolbasi, B., et al., *Chronic unpredictable stress disturbs the blood-testis barrier affecting*
422 *sperm parameters in mice.* Reprod Biomed Online, 2021. **42**(5): p. 983-995.
423 46. Asraf, K., et al., *Synergistic, long-term effects of glutamate dehydrogenase 1 deficiency*
424 *and mild stress on cognitive function and mPFC gene and miRNA expression.* Transl
425 Psychiatry, 2023. **13**(1): p. 248.
426 47. Muller, H.K., et al., *Differential expression of synaptic proteins after chronic restraint*
427 *stress in rat prefrontal cortex and hippocampus.* Brain Res, 2011. **1385**: p. 26-37.
428 48. McEwen, B.S., *Neurobiological and Systemic Effects of Chronic Stress.* Chronic Stress
429 (Thousand Oaks), 2017. **1**.
430 49. Mozhui, K., et al., *Strain differences in stress responsivity are associated with divergent*
431 *amygdala gene expression and glutamate-mediated neuronal excitability.* J Neurosci, 2010.
432 **30**(15): p. 5357-67.
433 50. Chen, C.C., et al., *Selective activation of parvalbumin interneurons prevents stress-induced*
434 *synapse loss and perceptual defects.* Mol Psychiatry, 2018. **23**(7): p. 1614-1625.
435 51. Stadelmann, C., et al., *Myelin in the Central Nervous System: Structure, Function, and*
436 *Pathology.* Physiol Rev, 2019. **99**(3): p. 1381-1431.
437 52. Gautam, A., et al., *Acute and chronic plasma metabolomic and liver transcriptomic stress*
438 *effects in a mouse model with features of post-traumatic stress disorder.* PLoS One, 2015.
439 **10**(1): p. e0117092.
440 53. Kuehner, J.N., et al., *Social defeat stress induces genome-wide 5mC and 5hmC alterations*
441 *in the mouse brain.* G3 (Bethesda), 2023. **13**(8).
442 54. Mingardi, J., et al., *Involvement of miR-135a-5p Downregulation in Acute and Chronic*
443 *Stress Response in the Prefrontal Cortex of Rats.* Int J Mol Sci, 2023. **24**(2).

55. Kosuth, J., et al., *Selection of Reliable Reference Genes for Analysis of Gene Expression in Spinal Cord during Rat Postnatal Development and after Injury.* Brain Sci, 2019. **10**(1).
56. Pelkey, K.A., et al., *Pentraxins Coordinate Excitatory Synapse Maturation and Circuit Integration of Parvalbumin Interneurons.* Neuron, 2016. **90**(3): p. 661.
57. Fan, R. and K.O. Lai, *Understanding how kinesin motor proteins regulate postsynaptic function in neuron.* FEBS J, 2022. **289**(8): p. 2128-2144.
58. Gerfen, C.R. and P.E. Sawchenko, *An anterograde neuroanatomical tracing method that shows the detailed morphology of neurons, their axons and terminals: immunohistochemical localization of an axonally transported plant lectin, Phaseolus vulgaris leucoagglutinin (PHA-L).* Brain Res, 1984. **290**(2): p. 219-38.
59. Frey, U. and R.G. Morris, *Synaptic tagging and long-term potentiation.* Nature, 1997. **385**(6616): p. 533-6.
60. Rangaraju, V., S. Tom Dieck, and E.M. Schuman, *Local translation in neuronal compartments: how local is local?* EMBO Rep, 2017. **18**(5): p. 693-711.
61. Issler, O., et al., *MicroRNA 135 is essential for chronic stress resiliency, antidepressant efficacy, and intact serotonergic activity.* Neuron, 2014. **83**(2): p. 344-360.
62. Jaffe, A.E., et al., *Decoding Shared Versus Divergent Transcriptomic Signatures Across Cortico-Amygdala Circuitry in PTSD and Depressive Disorders.* Am J Psychiatry, 2022. **179**(9): p. 673-686.
63. Ochi, S. and Y. Dwivedi, *Dissecting early life stress-induced adolescent depression through epigenomic approach.* Mol Psychiatry, 2023. **28**(1): p. 141-153.
64. McMurray, K.M.J., et al., *Identification of a novel, fast-acting GABAergic antidepressant.* Mol Psychiatry, 2018. **23**(2): p. 384-391.
65. Suminaite, D., D.A. Lyons, and M.R. Livesey, *Myelinated axon physiology and regulation of neural circuit function.* Glia, 2019. **67**(11): p. 2050-2062.
66. Pitman, R.K., et al., *Biological studies of post-traumatic stress disorder.* Nat Rev Neurosci, 2012. **13**(11): p. 769-87.
67. Roozendaal, B., J.M. Koolhaas, and B. Bohus, *The role of the central amygdala in stress and adaption.* Acta Physiol Scand Suppl, 1997. **640**: p. 51-4.

475 **Figure legends**

476 **Fig. 1：SLAM-seq for mouse brain cells by stereotactic injection of 4sU into the brain.**

477 **(a)** Schematic showing SLAM-seq procedure, including stereotactic 4sU injection, RNA
478 extraction, iodoacetamide (IAA) treatment, RNA sequencing and T-C conversion detection.

479 **(b)** Dot blot essay of RNA extracted from mouse brain labeled with 4sU for different durations.
480 Left to right: biotin-oligo (positive control); RNA samples extracted from mouse auditory
481 cortex with no 4sU injection (negative control); 2 h, 8 h, and 24 h after 4sU injection.

482 **(c)** TUNEL staining of brain slices for positive control (top panels), and brain slices with DMSO
483 (middle) and 4sU (bottom) injections in auditory cortex. Green signals denoted dead cells.

484 **(d)** Correlation of RNA levels extracted from DMSO (denoted as 4sU-) and 4sU (denoted as 4sU+)
485 injected auditory cortex samples. ρ, spearman correlation coefficient.

486

487 **Fig. 2：Identifying 4sU-labeled genes with SLAM-seq and match to different cell types**

488 **(a)** Time line showing stereotactic 4sU injection and brain extraction under baseline (BL)
489 condition. Shading demonstrates nascent mRNA that can be detected by SLAM-seq.

490 **(b)** T>C Conversion rates of total mRNA extracted from DMSO (n=5) and 4sU (n=4) injected
491 amygdala under baseline condition.

492 **(c)** Volcano plots showing T>C conversion rates of transcripts under baseline, with or without
493 4sU injection. Red dots represent transcripts with significant higher T>C conversion rates in
494 the 4sU+ group (FDR < 0.05 and $\log_2$FC > 1); blue dots represent transcripts with significant
495 lower T>C conversion rates in the 4sU+ group (FDR < 0.05 and $\log_2$FC < -1).

496 **(d)** T>C Conversion rates of marker genes for multiple neuron and glia cell types.

497

498 **Fig. 3：Transcriptome dynamics of mouse amygdala under acute stress.**

499 **(a)** Time line of acute stress experiment, including time points for 4sU injection and brain
500 extraction.

501 **(b)** Volcano plots showing T>C conversion rates of transcripts under AS, with or without 4sU
502 injection. Red dots represent transcripts with significant higher T>C conversion rates in the
503 4sU+ group (FDR < 0.05 and $\log_2$FC > 1); blue dots represent transcripts with significant lower
504 T>C conversion rates in the 4sU+ group (FDR < 0.05 and $\log_2$FC < -1).

505 **(c)** GO term analysis for genes detected by SLAM-seq.

506 **(d)** KEGG analysis for genes detected by SLAM-seq.

507 **(e)** Fold changes of T>C conversion rates for GABA and glutamate receptors detected by SLAM-
508 seq. Paired t-test, *** $P < 0.001$.

509 **(f)** Volcano plots showing differentially expressed genes (DEGs) under AS compared to BL. Red
510 dots represent significantly AS-upregulated genes (FDR < 0.1 and $\log_2FC > 0.1$); blue dots
511 represent significantly AS-downregulated genes (FDR<0.1 and $\log_2FC < -0.1$). ns, no
512 significant difference; up, significantly upregulated; down, significantly downregulated.

513 **(g)** Venn diagram showing intersection of AS-specific genes identified by SLAM-seq (red dots in
514 **b**) and RNA-seq (red dots in **f**).

515 **(h)** Fold changes of T>C conversion rates for 4sU+ vs. 4sU- (SLAM), and of expression levels for
516 AS vs. BL (DEG) of all overlapped genes in (**g**). Paired t-test, *** $P < 0.001$.

517 **(i)** Correlation between FC-DEG and expression levels of AS-upregulated genes in **3g**, with the
518 color and size of each data point denoting the significance level (FDR-SLAM) and fold change
519 (FC-SLAM) of each AS-upregulated gene.

520 **(j)** Distribution for expression levels of genes detected by SLAM-seq and RNA-seq under AS.
521 Two-sample Kolmogorov-Smirnov test, $p < 0.05$

522 **(k)** Significance levels of T>C conversion rates for 4sU+ vs. 4sU- (SLAM), and of expression
523 levels for AS vs. BL (DEG) of all overlapped genes in (**g**). Paired t-test, *** $P < 0.001$.

524

525 **Fig. 4：Transcriptome dynamics of mouse amygdala under chronic stress.**

526 **(a)** Time line of chronic stress experiment, including time points for 4sU injection and brain
527 extraction.

528 **(b)** Volcano plots showing T>C conversion rates of transcripts under CS, with or without 4sU
529 injection. Red dots represent transcripts with significant higher T>C conversion rates in the
530 4sU+ group (FDR < 0.05 and $\log_2FC > 1$); blue dots represent transcripts with significant lower
531 T>C conversion rates in the 4sU+ group (FDR < 0.05 and $\log_2FC < -1$).

532 **(c)** GO term analysis for genes detected by SLAM-seq.

533 **(d)** Volcano plots showing differentially expressed genes (DEGs) under CS compared to BL. Red
534 dots represent significantly AS-upregulated genes (FDR < 0.1 and $\log_2FC > 0.1$); blue dots
535 represent significantly AS-downregulated genes (FDR<0.1 and $\log_2FC < -0.1$).

536 **(e)** Venn diagram showing intersection of AS-specific genes identified by SLAM-seq (red dots in

537 **b**) and RNA-seq (red dots in **d**).

538 **(f)** Correlation between FC-DEG and expression levels of AS-upregulated genes in **e**, with the
539 color and size of each data point denoting the significance level (FDR-SLAM) and fold change
540 (FC-SLAM) of each CS-upregulated gene.

541 **(g)** Distribution for expression levels of genes detected by SLAM-seq and RNA-seq under CS.
542 Two-sample Kolmogorov-Smirnov test, $p < 0.05$.

543 **(h)** Fold changes of T>C conversion rates for 4sU+ vs. 4sU- (SLAM), and of expression levels for
544 AS vs. BL (DEG) of all overlapped genes in (**e**). Paired t-test, *** $P < 0.001$.

545 **(i)** Significance levels of T>C conversion rates for 4sU+ vs. 4sU- (SLAM), and of expression
546 levels for AS vs. BL (DEG) of all overlapped genes in (**e**). Paired t-test, * $P < 0.05$.

547

548 **Fig. 5：Comparison of AS and CS-associated genes.**

549 **(a)** Venn diagram showing intersections of genes identified by SLAM-seq under BL, AS and CS
550 conditions. Genes associated with synapse, postsynaptic plasticity, autophagy and myelination
551 are listed.

552 **(b)** GO term analysis for AS-specific genes.

553 **(c)** Fold changes of T>C conversion rates for GABA and glutamate receptors detected by SLAM-
554 seq under CS. Paired t-test, *** $P < 0.001$.

555 **(d)** GO term analysis for CS-specific genes.

556

Figure 1

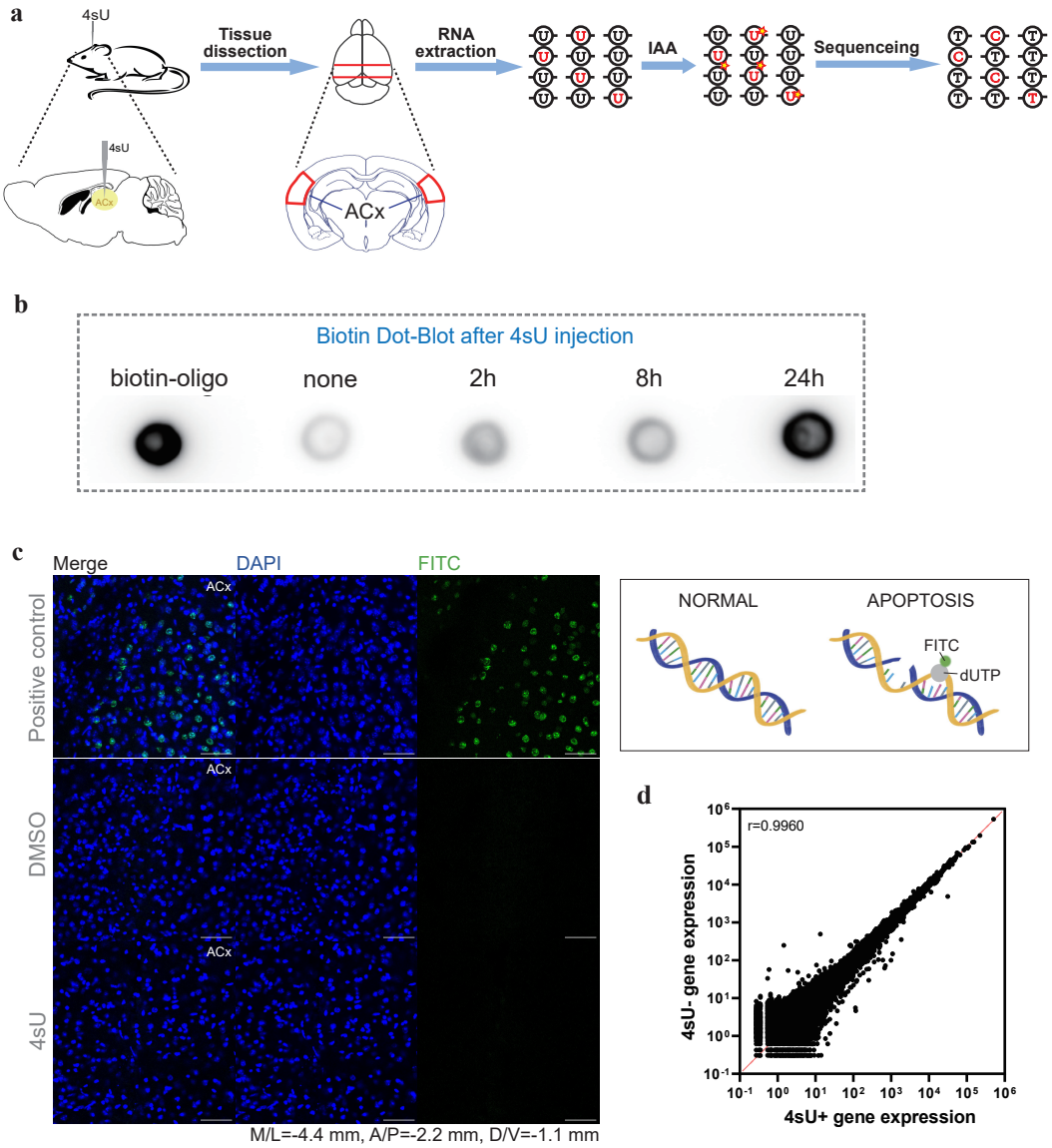
a
4sU
Tissue dissection
RNA extraction
IAA
Sequenceing
ACx
b
Biotin Dot-Blot after 4sU injection
biotin-oligo
none
2h
8h
24h
c
Merge
DAPI
FITC
Positive control
DMSO
4sU
ACx
M/L=-4.4 mm, A/P=-2.2 mm, D/V=-1.1 mm
NORMAL
APOPTOSIS
FITC
dUTP
d
r=0.9960
4sU- gene expression
4sU+ gene expression

Figure 2

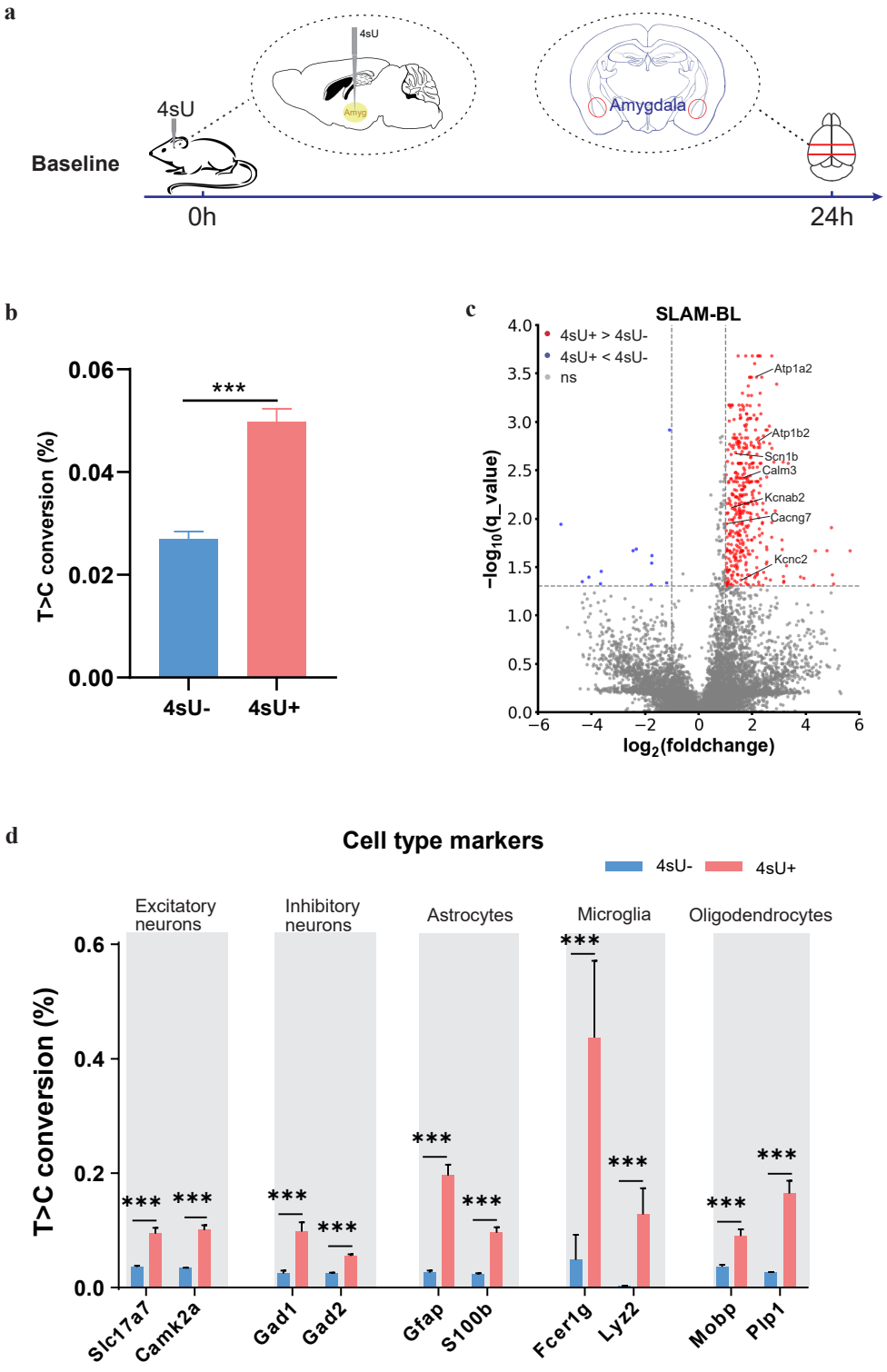
a
4sU
Baseline
0h
24h
Amygdala
b
T>C conversion (%)
0.06
0.04
0.02
0.00
***
4sU-
4sU+
c
SLAM-BL
4sU+ > 4sU-
4sU+ < 4sU-
ns
Atp1a2
Atp1b2
Scn1b
Calm3
Kcnab2
Cacng7
Kcnc2
−log10(q_value)
log2(foldchange)
d
Cell type markers
4sU-
4sU+
Excitatory neurons
Inhibitory neurons
Astrocytes
Microglia
Oligodendrocytes
T>C conversion (%)
Slc17a7
Camk2a
Gad1
Gad2
Gfap
S100b
Fcer1g
Lyz2
Mobp
Plp1

Figure 3

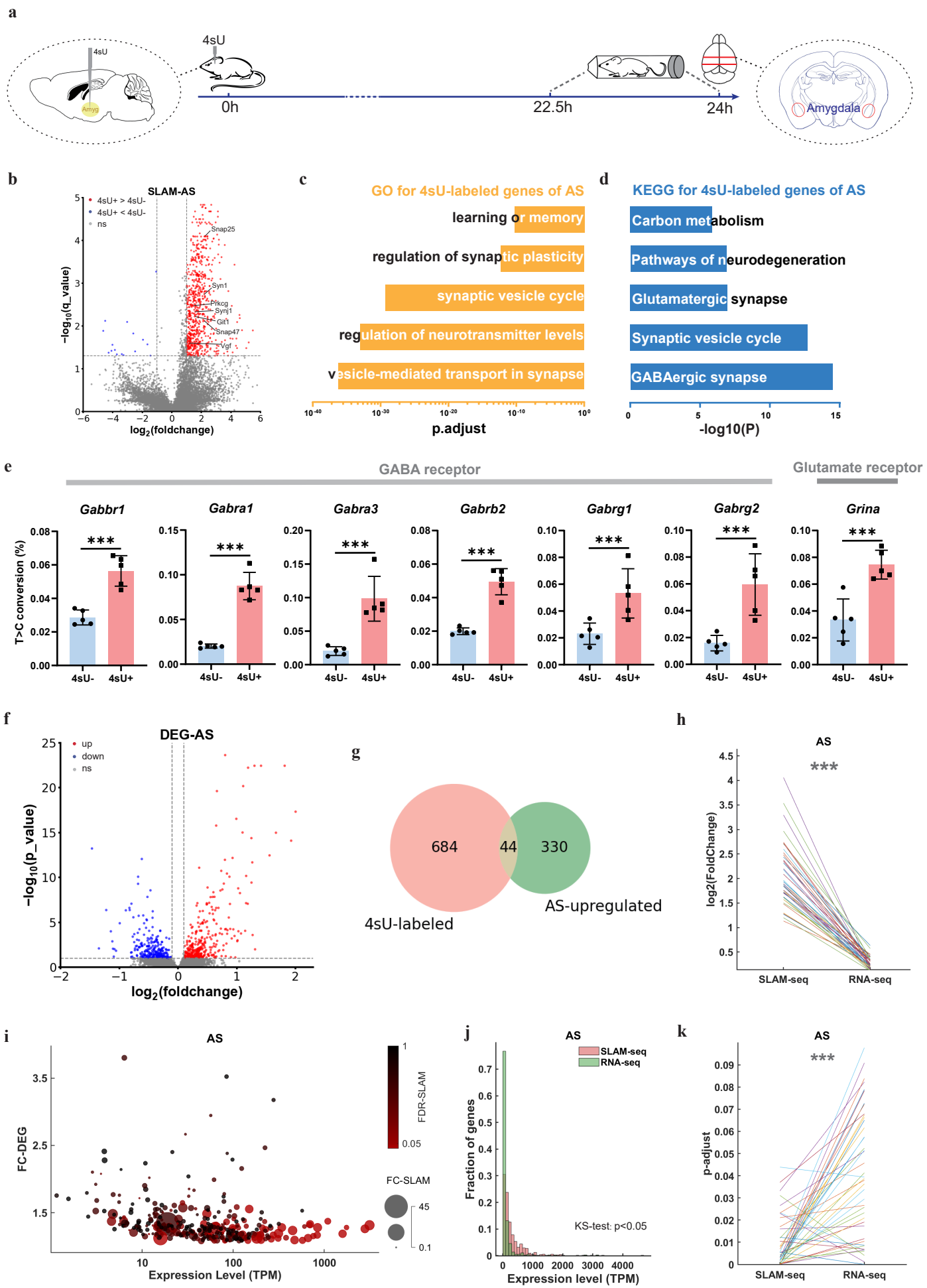
a
4sU
Amyg
4sU
0h
22.5h
24h
Amygdala
b
SLAM-AS
4sU+ > 4sU-
4sU+ < 4sU-
ns
Snap25
Syn1
Prkcg
Syn1
Git1
Snap47
Vgf
−log10(q_value)
log2(foldchange)
c
GO for 4sU-labeled genes of AS
learning or memory
regulation of synaptic plasticity
synaptic vesicle cycle
regulation of neurotransmitter levels
vesicle-mediated transport in synapse
p.adjust
d
KEGG for 4sU-labeled genes of AS
Carbon metabolism
Pathways of neurodegeneration
Glutamatergic synapse
Synaptic vesicle cycle
GABAergic synapse
-log10(P)
e
GABA receptor
Glutamate receptor
Gabbr1
Gabra1
Gabra3
Gabrb2
Gabrg1
Gabrg2
Grina
T>C conversion (%)
4sU-
4sU+
f
DEG-AS
up
down
ns
−log10(p_value)
log2(foldchange)
g
684
44
330
4sU-labeled
AS-upregulated
h
AS
log2(FoldChange)
SLAM-seq
RNA-seq
i
AS
FC-DEG
Expression Level (TPM)
FDR-SLAM
FC-SLAM
j
AS
SLAM-seq
RNA-seq
Fraction of genes
KS-test: p<0.05
Expression level (TPM)
k
AS
p-adjust
SLAM-seq
RNA-seq

Figure 4

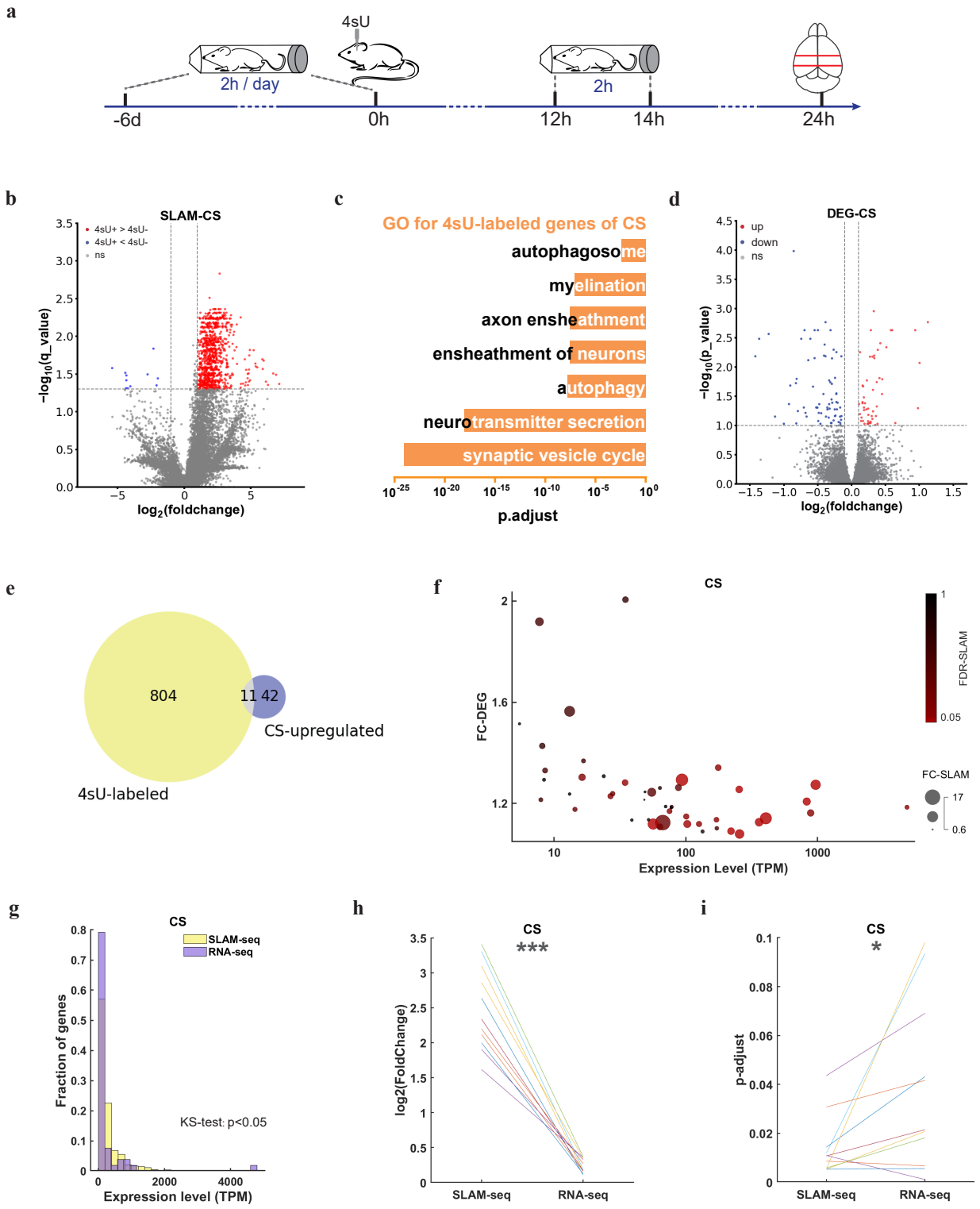
a
4sU
2h / day
2h
-6d
0h
12h
14h
24h
b
SLAM-CS
4sU+ > 4sU-
4sU+ < 4sU-
ns
−log10(q_value)
log2(foldchange)
c
GO for 4sU-labeled genes of CS
autophagosome
myelination
axon ensheathment
ensheathment of neurons
autophagy
neurotransmitter secretion
synaptic vesicle cycle
p.adjust
d
DEG-CS
up
down
ns
−log10(p_value)
log2(foldchange)
e
804
11
42
CS-upregulated
4sU-labeled
f
CS
FC-DEG
Expression Level (TPM)
FDR-SLAM
FC-SLAM
g
CS
SLAM-seq
RNA-seq
Fraction of genes
KS-test: p<0.05
Expression level (TPM)
h
CS
***
log2(FoldChange)
SLAM-seq
RNA-seq
i
CS
*
p-adjust
SLAM-seq
RNA-seq

Figure 5

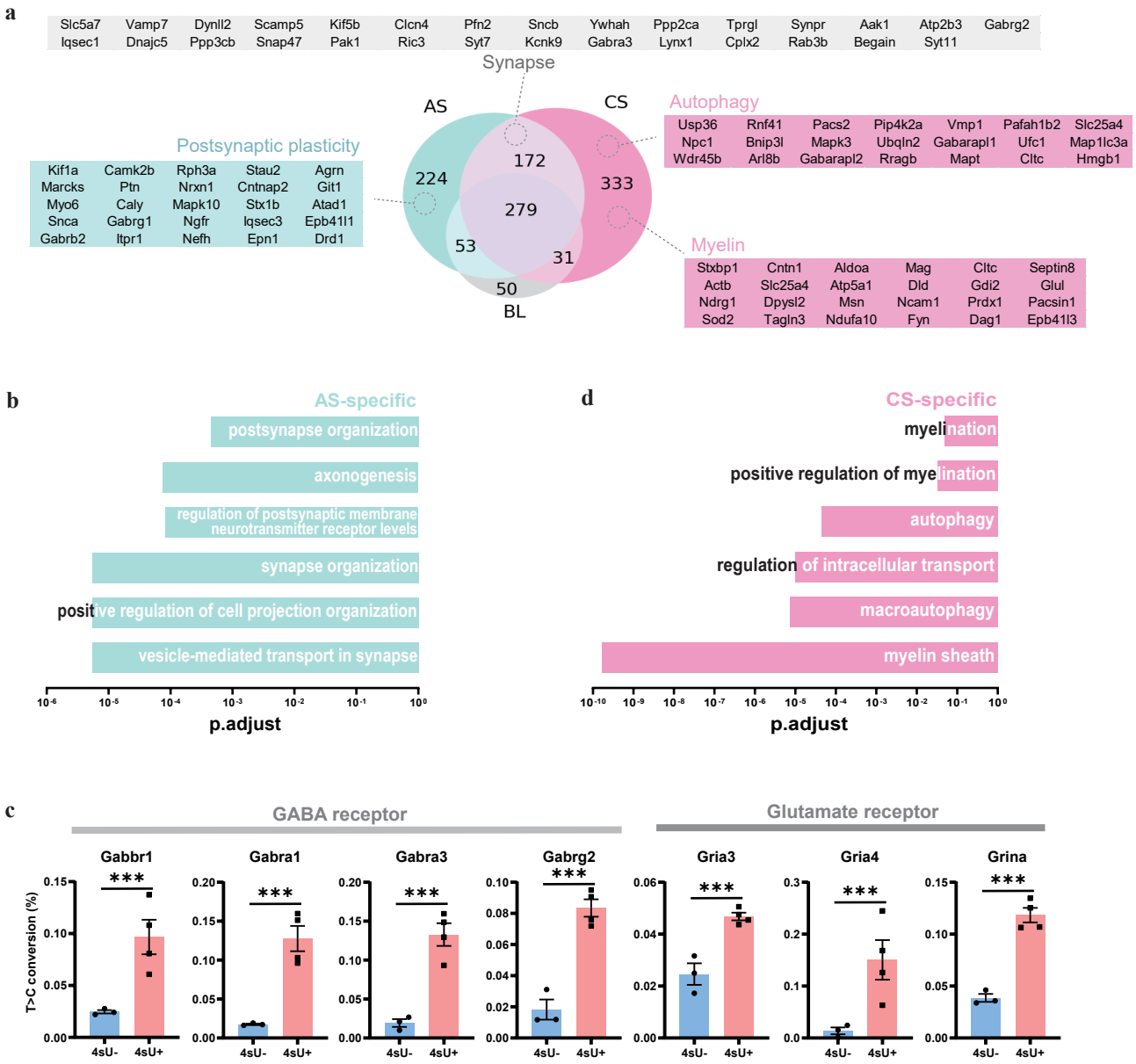
a
Slc5a7 Vamp7 Dynll2 Scamp5 Kif5b Clcn4 Pfn2 Sncb Ywhah Ppp2ca Tprgl Synpr Aak1 Atp2b3 Gabrg2
Iqsec1 Dnajc5 Ppp3cb Snap47 Pak1 Ric3 Syt7 Kcnk9 Gabra3 Lynx1 Cplx2 Rab3b Begain Syt11
Synapse
AS
CS
BL
224
172
279
333
53
31
50
Postsynaptic plasticity
Kif1a Camk2b Rph3a Stau2 Agrn
Marcks Ptn Nrxn1 Cntnap2 Git1
Myo6 Caly Mapk10 Stx1b Atad1
Snca Gabrg1 Ngfr Iqsec3 Epb41l1
Gabrb2 Itpr1 Nefh Epn1 Drd1
Autophagy
Usp36 Rnf41 Pacs2 Pip4k2a Vmp1 Pafah1b2 Slc25a4
Npc1 Bnip3l Mapk3 UbqIn2 Gabarapl1 Ufc1 Map1lc3a
Wdr45b Arl8b Gabarapl2 Rragb Mapt Cltc Hmgb1
Myelin
Stxbp1 Cntn1 Aldoa Mag Cltc Septin8
Actb Slc25a4 Atp5a1 Dld Gdi2 Glul
Ndrg1 Dpysl2 Msn Ncam1 Prdx1 Pacsin1
Sod2 Tagln3 Ndufa10 Fyn Dag1 Epb41l3
b
AS-specific
postsynapse organization
axonogenesis
regulation of postsynaptic membrane neurotransmitter receptor levels
synapse organization
positive regulation of cell projection organization
vesicle-mediated transport in synapse
10-6 10-5 10-4 10-3 10-2 10-1 100
p.adjust
d
CS-specific
myelination
positive regulation of myelination
autophagy
regulation of intracellular transport
macroautophagy
myelin sheath
10-10 10-9 10-8 10-7 10-6 10-5 10-4 10-3 10-2 10-1 100
p.adjust
c
GABA receptor
Glutamate receptor
Gabbr1 Gabra1 Gabra3 Gabrg2 Gria3 Gria4 Grina
T>C conversion (%)
***
4sU- 4sU+